The Journal of Neuroscience, August 15, 2002, 22(16):6991–7005

Signaling of Layer 1 and Whisker-Evoked Ca^{2+} and Na^{+} Action Potentials in Distal and Terminal Dendrites of Rat Neocortical Pyramidal Neurons *In Vitro* and *In Vivo*

Matthew E. Larkum[1] **and J. Julius Zhu**[1,2,3]

[1]*Department of Cell Physiology, Max Planck Institute for Medical Research, Heidelberg D-69120, Germany,* [2]*Cold Spring Harbor Laboratory, Cold Spring Harbor, New York 11724, and* [3]*Department of Pharmacology, University of Virginia School of Medicine, Charlottesville, Virginia 22908*

Dendritic regenerative potentials play an important role in integrating and amplifying synaptic inputs. To understand how distal synaptic inputs are integrated and amplified, we made multiple simultaneous (double, triple, or quadruple) and sequential (4–12 paired) recordings from different locations of single tufted layer 5 pyramidal neurons in the cortex *in vitro* and studied the spatial and temporal properties of their dendritic regenerative potential initial zone. Recordings from the soma and from trunk, primary, secondary, tertiary, and quaternary tuft branches of the apical dendrite of these neurons reveal a spatially restricted low-threshold zone ~550–900 μm from the soma for Ca^{2+}-dependent regenerative potentials. Dendritic regenerative potentials initiated in this zone have a clearly defined threshold and a refractory period, and they can propagate actively along the dendrite before evoking somatic action potentials. The detailed biophysical characterization of this dendritic action potential initiation zone allowed for the further investigation of dendritic potentials in the intact brain and their roles in information processing. By making whole-cell recordings from the soma and varied locations along the apical dendrite of 53 morphologically identified layer 5 pyramidal neurons in anesthetized rats, we found that three of the dendritic potentials characterized *in vitro* could be induced by spontaneous or whisker inputs *in vivo*. Thus layer 5 pyramidal neurons of the rat neocortex have a spatially restricted low-threshold zone in the apical dendrite, the activation or interaction of which with the axonal action potential initiation zone is responsible for multiple forms of regenerative potentials critical for integrating and amplifying sensory and modulatory inputs.

Key words: rat; somatosensory; excitation; inhibition; synaptic integration; development; attention; synaptic plasticity

In 1951, Chang recorded a slow potential in the neocortex and proposed that the apical dendrite of pyramidal neurons can support regenerative potentials (Chang, 1951a,b). This proposal remained contentious for decades in the absence of direct intracellular recordings from the apical dendrite (Bishop and Clare, 1953; Purpura and Grundfest, 1956). More recent work confirms the existence of active conductances in the apical dendrite of pyramidal neurons (Spencer and Kandel, 1961; Wong et al., 1979; Benardo et al., 1982; Turner et al., 1991; Amitai et al., 1993; Kim and Connors, 1993; Regehr et al., 1993; Magee and Johnston, 1995a; Schwindt and Crill, 1995; Golding and Spruston, 1998). It is now clear that Ca^{2+}-dependent regenerative potentials can be initiated in the distal apical dendrite of pyramidal neurons (Schiller et al., 1997; Golding et al., 1999; Zhu, 2000; Oakley et al., 2001). Initiation of dendritic regenerative potentials can have profound effects on synaptic integration and synaptic plasticity (for review, see Hausser et al., 2000; Magee, 2000; Reyes, 2001). However, the threshold for activation of Ca^{2+} potentials, its time-dependent properties, and the spatial extent of the dendritic initiation zone remained to be elucidated.

Using multiple simultaneous and sequential recordings from the soma and different locations of the apical dendrite of single layer 5 pyramidal neurons of adult rats [more than postnatal day 42 (P42)], we mapped the electrical excitability of the apical dendrite. We found that adult layer 5 pyramidal neurons have a low-threshold zone in the distal apical dendrite for initiating predominantly Ca^{2+}-dependent regenerative potentials. The regenerative dendritic potentials had a threshold and a refractory period and could propagate without decrement along the apical dendrite. The results indicate that adult layer 5 pyramidal cells have an additional site for amplification and integration of synaptic inputs.

The dendritic action potential initiation zone of layer 5 pyramidal neurons can interact with the axonal action potential initiation zone. In addition to the dendritically initiated regenerative potentials, several other regenerative potentials have been observed, and their biophysical properties have been characterized by previous *in vitro* studies (Larkum et al., 1999a,b, 2001; Zhu, 2000). However, dendritic regenerative potentials are much less studied *in vivo*; only a small number of dendritic recordings have been made from the apical dendrite of layer 5 pyramidal neurons in the intact brain (Helmchen et al., 1999; Zhu and Connors, 1999). So far, it is still unclear whether the multiple forms of regenerative potentials observed in *in vitro* preparations occur *in vivo*. In this study we made whole-cell recordings from the soma and varied locations along the apical dendrite of layer 5 pyramidal

Received Jan. 23, 2002; revised May 28, 2002; accepted May 29, 2002.

This work was supported in part by the Alzheimer's Association, the Fraxa Medical Research Foundation, and the Max Planck Society. J.J.Z. is a Naples Investigator of the National Alliance for Research on Schizophrenia and Depression Foundation. We thank Professor Bert Sakmann for his support and discussions; Drs. Hsiang-Tung Chang, Alon Krongreen, Troy Margrie, and Arnd Roth for their helpful comments; and Drs. Katharina Kaiser and Yi Qin for help in some experiments and histological processing.

Correspondence should be addressed to Dr. J. Julius Zhu, Department of Pharmacology, University of Virginia School of Medicine, 1300 Jefferson Park Avenue, Charlottesville, VA 22908. E-mail: jjzhu@virginia.edu.

Copyright © 2002 Society for Neuroscience 0270-6474/02/226991-15$15.00/0

neurons in anesthetized rats. We found that three of the regenerative potentials characterized *in vitro* could be evoked by spontaneous and whisker inputs. Although some of the biophysical characteristics of the regenerative potentials remained unchanged *in vivo*, others were notably different in the intact brain.

MATERIALS AND METHODS

In vitro *brain slice preparation.* Brain slices of the somatosensory neocortex were prepared from 6- to 8-week-old (180–280 gm) Wistar rats unless stated otherwise. The main procedure followed a previous study (Zhu, 2000). In brief, animals were anesthetized deeply by halothane and decapitated. The brain was removed quickly and placed into cold (0–4°C) oxygenated physiological solution containing (in mM): 125 NaCl, 2.5 KCl, 1.25 NaH_2PO_4, 25 $NaHCO_3$, 1 $MgCl_2$, 25 dextrose, and 2 $CaCl_2$, pH 7.4. Sagittal slices 250–300 μm thick were cut from the tissue blocks with a microslicer. These slices were kept at 37.0 ± 0.5°C in oxygenated physiological solution for ~1 hr before recordings were made. During the recording the slices were submerged in a chamber and stabilized with a fine nylon net attached to a platinum ring. The chamber was perfused with oxygenated physiological solution, the half-time for the bath solution exchange being ~6 sec. As reported previously (Chang, 1952), we found that the initiation and propagation of dendritic regenerative potentials were compromised when neurons were recorded at room temperature, attributable presumably to the high sensitivity of calcium channel kinetics to the temperature (Coulter et al., 1989; McAllister-Williams and Kelly, 1995). Thus all recordings reported in this study were performed with the temperature of the bath solution in the recording chamber maintained at 35.0 ± 0.5°C. All antagonists were bath applied.

In vitro *electrophysiology.* Double, triple, quadruple, and multiple recordings were made on single identified layer 5 pyramidal neurons by using infrared illumination combined with differential interference contrast optics. Somatic (5–10 MΩ) and dendritic (10–25 MΩ) recording pipettes were filled with standard intracellular solution containing (in mM): 115 potassium gluconate, 10 HEPES, 2 $MgCl_2$, 2 Mg-ATP, 2 Na_2ATP, 0.3 GTP, and 20 KCl plus 0.25% biocytin, pH 7.3. Dendritic tufts branches were identified and recorded as described previously (Zhu, 2000). Whole-cell recordings were made with up to four Axoclamp-2B amplifiers (Axon Instruments, Foster City, CA). Whenever necessary, the output of recording head stages was monitored on an oscilloscope so that the electrode capacitance compensation could be made in the discontinuous current-clamp mode. A 10 mV liquid junction potential was subtracted from all membrane potentials.

In vitro *synaptic stimulation.* Extracellular synaptic stimulation was made by a concentric bipolar electrode with single voltage pulses (200 μsec, up to 40 V, 0.25 Hz). The stimulating electrode was placed at the border of layer 1 and layer 2, ~1200–1500 μm lateral from the cells that were recorded. Slices were cut between the stimulating electrode and the cells with a surgical scraper (from the middle layer 2 to white matter; 300–500 μm lateral from the cells). This arrangement made it possible to activate layer 1/2 synaptic inputs more selectively (cf. Cauller and Connors, 1994). Sometimes the stimulating electrode was placed in the border of layer 6 and white matter, ~100–300 μm lateral from the cells that were recorded, to activate layer 4/5 inputs of layer 5 pyramidal neurons.

In vivo *animal preparation.* As described previously (Zhu and Connors, 1999), 6- to 8-week-old (180–280 gm) Wistar rats were anesthetized initially by an intraperitoneal injection of pentobarbital sodium (60 mg/kg). Supplemental doses (10 mg/kg) of pentobarbital were given as needed to keep animals free from pain reflexes and in a state of slow-wave general anesthesia, as determined by monitoring the cortical electroencephalogram (EEG). All pressure points and incised tissues were infiltrated with lidocaine. Body temperature (rectal) was monitored and maintained within the normal range (37.2 ± 0.3°C). During the physiological investigation the animals were placed in a stereotaxic frame. A hole ~3 × 4 mm was opened above the right somatosensory cortex according to the stereotaxic coordinates (Chapin and Lin, 1984). The dura was opened just before the electrode penetrations. Electrodes typically were arranged to penetrate the barrel cortex at ~60° against the surface plane, aiming at the center of the mystacial vibrissal barrel cortex. At the end of each neuronal recording the subpial depth of the cell was estimated from the distance that the micromanipulator had advanced, taking into account the angle that the electrode formed with the surface of the barrel cortex. The estimation matched well with the reconstructed electrode penetration pathway that was revealed after histology processing (see below).

In vivo *electrophysiology.* Whole-cell recordings from the soma and dendrite of cortical neurons were made blindly, as described in a previous report (Zhu and Connors, 1999). Long-taper patch electrodes were made from borosilicate tubing, and their resistances were initially 7–15 MΩ. The same intracellular solution used in *in vitro* experiments was used. A 10 mV liquid junction potential was subtracted from all membrane potentials to facilitate the comparison of *in vitro* and *in vivo* data. To obtain whole cell recordings, we advanced electrodes into the brain while pulsing with 0.1 nA current steps of 200 msec duration. Positive pressure (75–150 mbar) was applied constantly to the pipette while it was being advanced. Once in a while, a short pulse of high pressure (300–450 mbar) was applied to inject biocytin and stain cell debris along the penetration pathway. When a sudden increase in electrode resistance was evident, gentle suction was applied to obtain a seal resistance of ≥1 GΩ. The patch of the membrane was broken by applying more negative pressure to obtain a whole-cell configuration. All *in vivo* data were collected when the access resistance of recordings was <50 MΩ. An Axoclamp-2B amplifier (Axon Instruments) was used for intracellular recordings. The electrode capacitance compensation was made in discontinuous current-clamp mode, with the head stage output continuously monitored on a second oscilloscope. A satisfactory capacitance compensation was achieved in most recordings (with the exception of recordings from the soma and proximal dendrite of a few layer 5 pyramidal neurons).

In vivo *whisker and synaptic stimulation.* Single whiskers on the contralateral face were deflected briefly for a short distance (40–200 μm) with a piezoelectric stimulator placed adjacent to the whisker and activated by single brief voltage pulses (0.3–0.5 msec, 2–10 V, 0.25 Hz) (cf. Dykes et al., 1977; Simons, 1983). Extracellular synaptic stimulation was made by a concentric bipolar electrode with single voltage pulses (200 μsec, up to 25 V, 0.25 Hz). The stimulating electrode was placed on the cortical surface ~1000–2000 μm lateral from the electrode penetration site to activate layer 1/2 synaptic inputs more selectively (cf. Chang, 1952).

Histology. After *in vitro* recordings the slices were fixed by immersion in 4% paraformaldehyde in 0.1 M phosphate buffer. After *in vivo* recordings a small block of tissue, including the recorded cell, was removed from the brain and immersion-fixed with 4% paraformaldehyde in 0.1 M phosphate buffer. Later, the tissue blocks were sectioned 250 μm thick with a microslicer. Tissue sections from *in vitro* and *in vivo* experiments were processed with the avidin-biotin-peroxidase method to reveal cell morphology. Cells then were drawn with the aid of a microscope equipped with a computerized reconstruction system (Neurolucida; MicroBrightField, Colchester, VT). Only the data from the morphologically identified layer 5 pyramidal neurons were included in this report. For *in vivo* experiments, electrode penetration pathways were reconstructed on the basis of the biocytin staining of cell debris observed along the electrode penetration tracks (see Figs. 9–11). Then the exact site at the soma or apical dendrite of layer 5 pyramidal neurons at which the recordings were made was determined accordingly.

The threshold of dendritic regenerative potentials was determined by increasing stimuli with small steps (0.1 nA or 0.2 V). The threshold potential and duration of regenerative events were measured at their threshold point. All results are reported as the means ± SEM. Statistical differences of the means were determined by using paired Student's *t* test unless stated otherwise. The level of significance was set at $p < 0.05$.

RESULTS

Initiation of regular and burst patterns of action potentials in thick-tufted L5 neurons

With dual and triple whole-cell voltage recordings made from the same neuron (Fig. 1*A*) and depending on where in the neurons the dendritic current was injected, two major types of action potential patterns were evoked after (relatively long, 500 msec) rectangular current injections. Suprathreshold dendritic current injection always generated a regenerative potential in the dendrite and a burst of somatic Na^+ action potentials in the soma, whereas prolonged somatic current injection evoked action potentials occurring in either a burst pattern ($n = 21$) or a regular pattern ($n = 22$) in the soma. Figure 1*B,C* shows an example from a regular-spiking cell with somatic-injected current (RS; for def-

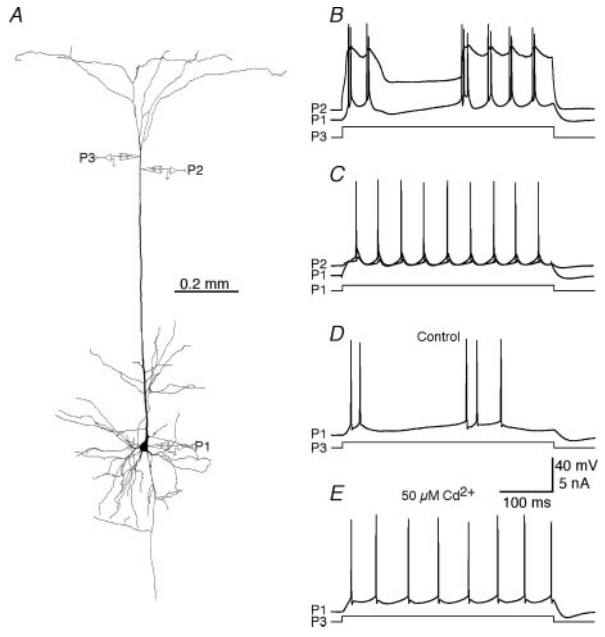

Figure 1. Burst and regular patterns of axonal action potentials evoked in the same neurons depend on the site of current injection. *A*, Reconstruction of a thick-tufted L5 pyramidal neuron. The schematic drawing of recording pipettes indicates the locations of the dendritic (908 and 868 μm distal from the soma for *P3* and *P2*, respectively) and somatic recordings. The length of the apical dendrite was 1279 μm. *B*, "Burst-like" axonally induced action potential pattern after dendritic current injection in the neuron, recorded with somatic pipette. The dendritic pipette recorded a Ca^{2+}-dependent regenerative potential. *C*, "Regular" axonal action potential pattern after somatic current injection in the same neuron, recorded with somatic pipette. The dendritic pipette recorded an attenuated pattern of somatic action potentials. Note that the *top traces* show dendritic responses, whereas the *bottom traces* show somatic responses (similarly in the following figures). The resting membrane potentials at the very distal dendrite, proximal distal dendrite, and soma were −72, −73, and −76 mV, respectively. *D*, Burst-like axonally induced action potential pattern after dendritic current injection in another neuron, recorded with somatic pipette. The locations of the dendritic recordings were 573 and 504 μm distal from the soma for *P3* and *P2*, respectively. The length of the apical dendrite was 1220 μm. *E*, Bath application of 50 μM Cd^{2+} transformed the burst firing pattern in the soma into the regular firing pattern. Dendritic recording traces are not shown in *D* and *E*. The resting membrane potentials at the very distal dendrite, proximal distal dendrite, and soma were −73, −75, and −81 mV, respectively.

inition, see Connors and Gutnick, 1990). The neuron responded to dendritic current injection with a burst of Na^+ action potentials (Fig. 1*B*), whereas somatic current injection caused a tonic firing of Na^+ action potentials (Fig. 1*C*) (cf. Wong and Stewart, 1992; Schwindt and Crill, 1998).

The difference between the patterns of somatic action potentials evoked by somatic and dendritic current injections was reduced or abolished in the presence of 50 μM Cd^{2+}, a blocker of Ca^{2+} channels ($n = 4$) (Fig. 1*D,E*, respectively). This result suggests that Ca^{2+} conductance can play a crucial role in the generation of bursts of action potentials at the soma and is consistent with our previous finding that the activation of dendritic Ca^{2+}-dependent regenerative potentials can dominate the output discharge pattern of the neuron (Zhu, 2000; Larkum et al., 2001). To understand exactly what mechanisms led to this dendritic influence, we investigated in more detail the biophysical properties of this initiation zone in the distal dendrite underlying the Ca^{2+}-dependent regenerative potential by using multiple simultaneous and sequential recordings along the apical dendrite and the soma. Our main goals were to characterize the potentials generated in this region by using the classical descriptive parameters for action potentials in all neurons: major ion conductances, threshold, refractory period, and propagation, which are crucial for us to understand how distal synaptic inputs are integrated.

Temporal properties of dendritic action potential initiation zone

When a relatively short (50 msec) step-depolarizing current pulse was injected into one of the tuft branches (Fig. 2*A*), it invariably evoked a slow regenerative potential with several peaks and dips that was mediated mainly by a Ca^{2+} conductance (Schiller et al., 1997; Zhu, 2000; Larkum et al., 2001). Concomitant with the dendritic regenerative potential, two to four Na^+ action potentials were recorded at the somatic pipette. Characteristically, the dendritic potential preceded the first somatic action potential in a burst, and all somatic action potentials propagated back into the dendritic arbor to induce depolarizing peaks riding on the top of the dendritic regenerative potential. Unlike P28–P32 neurons (Schiller et al., 1997; Zhu, 2000), rectangular current pulse (50 msec) injection evoked both dendritic regenerative potentials and somatic action potentials in adult neurons even at threshold. Dendritic potentials were initiated in an all-or-none manner with a clear threshold, and they overshot 0 mV ($n = 35$) (Fig. 2*B*). Dendritic regenerative potentials lasted much longer than Na^+ action potentials and ranged from 30 to 80 msec with a mean duration of 56.5 ± 12.6 msec ($n = 35$). The duration of dendritic potentials was not correlated with the number of Na^+-dependent action potentials recorded in the soma (2–4 action potentials; $r = 0.097$; ANOVA; $p > 0.5$).

Dendritic regenerative potentials, when evoked by current injection (50 msec at threshold intensity), had a relatively long refractory period. Paired pulse injection with varying interpulse intervals showed that the second depolarizing current pulse (50 msec) failed to evoke a regenerative potential if the interval between the two pulses was too short, the relative refractory period being ~250 msec (Fig. 2*C,F*). During the relative refractory period the time course of dendritic potentials was altered, and the leading peak appeared not to be fully regenerative, although a burst of Na^+ action potentials still could be evoked, followed by the typical plateau-like dendritic potential (Fig. 2*D*). The duration of the refractory period decreased with increasing amplitude of the depolarizing current (Fig. 2*E,F*), the absolute refractory period under these conditions being ~50 msec ($n = 7$) (Fig. 2*F*).

Spatial properties of dendritic action potential initiation zone

To map the spatial extent of excitability in the distal dendrites, we made multiple sequential recordings from different locations along the apical dendrite. A second pipette recording was always placed at the soma of the same pyramidal neuron (8–12 sequential paired recordings, $n = 4$; 4–7 sequential paired recordings, $n = 4$) (Fig. 3*A*). We found that a short (50 msec) current pulse injection into the proximal dendritic trunk initiated action potentials first at the soma (data not shown). Current pulse injections into the middle portion of the apical dendritic trunk showed that the initiation of regenerative potentials depended on the intensity of stimulation. At threshold, the somatic action potential preceded the dendritic regenerative potential (Fig. 3*B*). Suprathreshold stimulation evoked a Ca^{2+}-dependent dendritic regenerative potential and a burst of axonal action potentials. The leading

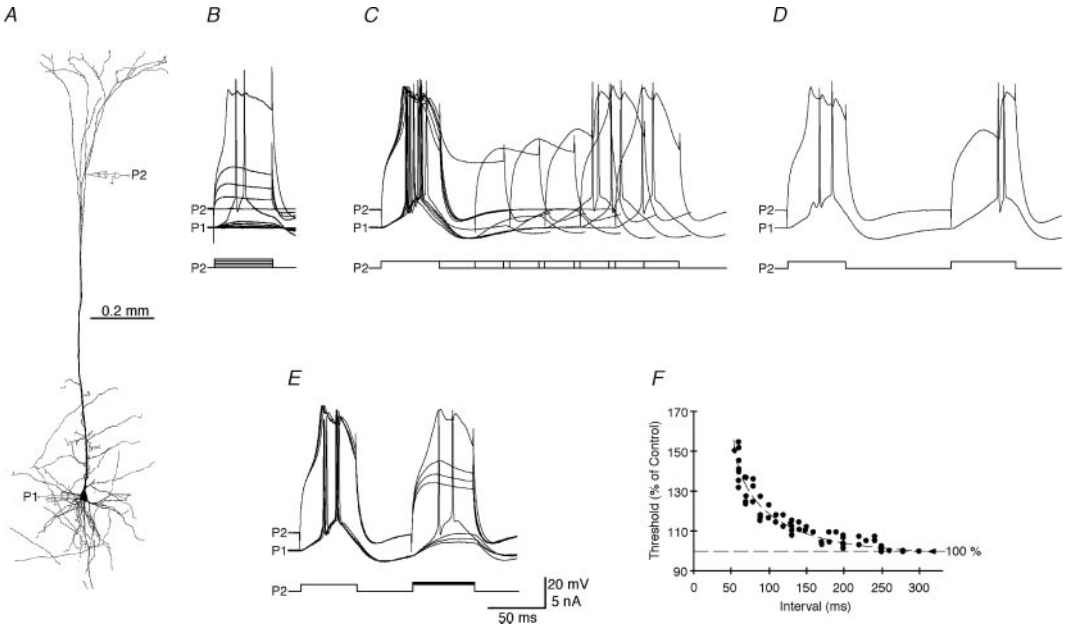

Figure 2. Duration and refractory period of regenerative potentials in the apical dendritic tuft neurons evoked by current pulse injection. *A*, Reconstruction of a biocytin-stained pyramidal neuron. The schematic drawing of recording pipettes indicates the location of the dendritic (981 μm distal from the soma; secondary tufts) and somatic recordings. The length of the apical dendrite was 1387 μm. *B*, All-or-none regenerative potentials evoked by depolarizing current injections into the dendrite of neuron. *C*, Paired depolarizing current injections at the dendritic electrode separated by varying time periods indicating the refractory period of dendritic regenerative potentials. The recordings with the altered regenerative potential are shown separated in *D*. *E*, Increasing the intensity of the second current pulse could evoke the regenerative potentials at a higher threshold. The calibration applies in *B–E*. *F*, Plotting threshold for the second regenerative potential against the interval between the two pulses revealed the refractory period of regenerative potentials. The *data points* were obtained from seven different neurons and were fit arbitrarily by an inverse function. The resting membrane potentials at the soma and dendrite were −78 and −69 mV, respectively.

depolarization of the dendritic potential preceded the somatic action potential (Fig. 3*C*). The results are consistent with the previous studies (Stuart and Sakmann, 1994; Stuart et al., 1997) (see also Chen et al., 1997). Finally, when current was injected into the distal dendritic trunk (686 ± 62 μm distal to the soma; $n = 8$) or in the primary or in the secondary dendritic tufts, a Ca^{2+}-dependent dendritic regenerative potential was initiated at threshold concomitant with a burst of somatic action potentials (Fig. 3*D*).

The threshold intensity for the initiation of regenerative dendritic potentials showed a progressive decrease in the distal dendrite and a progressive increase for somatic action potential initiation as a function of distance from the soma (Fig. 3*E–G*). These results indicate that, in the apical dendrites close to the bifurcation region of layer 5 pyramidal neurons with typical dendritic morphology, the threshold for the initiation of a dendritic regenerative potential is lower than that for the initiation of an axonal action potential.

Active propagation and spread of dendritic regenerative potentials

To determine how far regenerative potentials actively travel along the apical dendrite, we made simultaneous dendritic recordings in the dendritic tuft and distal dendritic trunk. Because the low-threshold region extended over a length estimated to be ~200–400 μm (Fig. 3*E,F*), we tested how a dendritic regenerative potential, once initiated, traveled within this region toward the soma. For this we made triple or quadruple recordings from the apical dendrite and soma (Fig. 4). The distal dendritic pipette was used to elicit and to record the dendritic depolarizing potentials in the dendritic tuft, whereas the proximal dendritic pipette or pipettes were used to measure the degree of attenuation of the dendritic depolarizing potentials in the distal dendritic trunk.

The thresholds for initiating the Ca^{2+}-dependent dendritic regenerative potentials in the primary tuft (699 ± 24 μm; $n = 7$) and distal dendritic trunk (588 ± 23 μm; $n = 7$) were the same (−48.7 ± 1.6 vs −48.0 ± 1.9 mV; $n = 7$; $p = 0.65$) (Fig. 4*B,C*). During the forward propagation from the primary tuft to distal dendritic trunk, the amplitude of regenerative potentials changed little (76.0 ± 2.3 vs 73.1 ± 1.6 mV; $n = 7$; $p = 0.13$) (Fig. 4*D*). These results are consistent with the presence of an extended low-threshold zone around the main branch point for the initiation of dendritic regenerative potentials (Fig. 3*E,F*). Propagation of the dendritic potentials in the proximal trunk was more variable. In some layer 5 pyramidal neurons the dendritic regenerative potentials transformed into graded potentials in the proximal trunk, which still could produce somatic action potentials (Fig. 4*E*). In other neurons they actively propagated into the proximal trunk, particularly when they were depolarized (Fig. 4*F*) (see also Larkum et al., 2001).

The threshold for the initiation of regenerative potentials appeared to increase toward the distal dendritic tips (Fig. 3*E,F*). To examine the distal extent of the active dendritic zone and to study the initiation and propagation of regenerative potentials in the terminal dendrite, we made dual simultaneous recordings from the primary ($n = 7$) and tertiary ($n = 5$) or quaternary ($n = 2$) tuft branches of the same pyramidal neurons (Fig. 5*A*). The average distance of the recordings at the primary tufts from the soma was 764 ± 22 μm ($n = 7$), whereas that of the recordings at the tertiary and quaternary tufts was 939 ± 32 μm ($n = 7$). The resting membrane potential in the tertiary and quaternary tufts

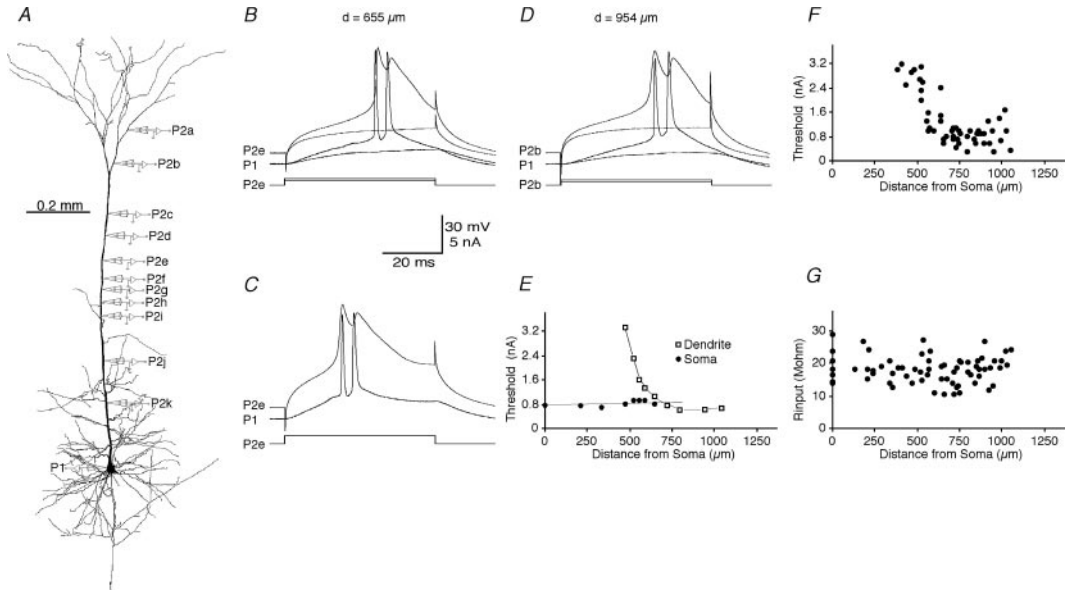

Figure 3. Thresholds of regenerative potentials along the apical dendrite. *A*, Schematic drawing of the recording pipettes indicates the locations of the dendritic (1055, 954, 801, 753, 655, 600, 564, 527, 482, 336, and 214 μm distal from the soma) and somatic recordings in 11 dual recordings from the same cell. Note that the dendritic recordings were obtained in random order. The length of the apical dendrite was 1367 μm. *B*, Somatic action potentials started earlier than the dendritic regenerative potentials in response to the threshold current injection at the dendrite 655 μm from the soma. *C*, At a higher current intensity the dendritic regenerative potentials were elicited before the somatic action potentials. *D*, At 954 μm from the soma the dendritic regenerative potentials always started first. The calibration applies to *B–D*. *E*, Plots of thresholds for somatic action potentials (*filled circles*) and for dendritic regenerative potentials (in the cases in which the dendritic potentials preceded the somatic action potentials; *open squares*) as a function of distance from the soma. The resting membrane potential at the soma was −78 mV. A regression line is fit to the somatic thresholds. The resting membrane potentials at the dendrite from distal to proximal were −69, −69, −70, −74, −75, −76, −77, −78, −78, −78, and −78 mV, respectively. *F, G*, Plots of threshold for dendritic regenerative potentials (*F*) or input resistance (*G*) at the different locations of the dendrites of eight different neurons as a function of distance from the soma.

was more depolarized than that in the primary tufts (−66.4 ± 1.2 vs −70.6 ± 0.6 mV; $n = 7$; $p < 0.005$). The tertiary and quaternary tufts also had a higher input resistance than the primary tufts (26.9 ± 1.8 vs 13.7 ± 1.3 MΩ; $n = 7$; $p < 0.0005$). The membranes of tertiary and quaternary tufts were less excitable; the depolarization required to evoke a regenerative potential in the tertiary or quaternary tufts was significantly higher than that in the primary tufts (−26.7 ± 3.6 vs −46.6 ± 1.4 mV; $n = 7$; $p < 0.001$) (Fig. 5*B,D*). Consistent with this observation, we found that, regardless of the pipette through which the depolarizing current was injected, the Ca^{2+}-dependent dendritic regenerative potentials always were initiated first at the primary tufts and then propagated to the tertiary and quaternary tufts ($n = 7$) (Fig. 5*C*). During the backward propagation from the primary tufts to the tertiary and quaternary tufts, the amplitude of the regenerative potentials was attenuated by ~25% (81.7 ± 0.6 vs 61.6 ± 3.7 mV; $n = 7$; $p < 0.005$) (Fig. 5*B,E*). The results thus indicate a low-threshold zone at the bifurcation region for the initiation of regenerative potentials, which propagate both toward the soma and away from the soma into the distal dendritic tips.

Initiation of dendritic regenerative potentials by layer 1 synaptic stimulation *in vitro*

Initiation of dendritic regenerative potentials depends strongly on the size and time course of the current injected in the dendrite (Larkum et al., 2001). It was therefore important to know what kind of dendritic potentials might be generated by synaptically evoked inputs, which differ from injected current in many aspects, including size and time course. We evoked synaptic inputs in layer 5 pyramidal neurons by extracellular stimulation. Extracellular stimulation of afferent fibers in layer 1 could evoke a Ca^{2+}-dependent dendritic potential followed by a burst of action potentials in the soma ($n = 16$) (Fig. 6). In younger (P14–P28) pyramidal cells, dendritically initiated regenerative potentials at threshold intensity were restricted mostly to the dendritic tufts, and it was only after higher-than-threshold stimulation intensity that the dendritic depolarization preceded the burst of somatic action potentials (Schiller et al., 1997; Zhu, 2000). We ruled out any washout effects of whole-cell recording that might cause an altered excitability by synaptic stimulation in layer 1 by recording dendritic and somatic potentials first in a cell-attached configuration ($n = 5$). Stimulation within layer 1 evoked large dendritic EPSPs in the tufts, whereas the depolarization at the soma was strongly attenuated (Fig. 6*B*). Increasing stimulation intensity eventually evoked a regenerative potential in the distal tuft dendrites and simultaneously a burst of two to three Na^+ action potentials at the soma (Fig. 6*B,C*). Subsequent whole-cell intracellular voltage recordings at the same dendritic and somatic locations confirmed that the synaptic stimulation evoked a Ca^{2+}-dependent regenerative potential in the dendritic tufts and a burst of action potentials in the soma (Fig. 6*D,E*), indicating that the whole-cell configuration did not alter the regenerative properties of the dendrite in these respects.

The Ca^{2+}-dependent dendritic regenerative potentials evoked by synaptic stimulation were shorter than those evoked by current injection. On average, the duration of the synaptically evoked dendritic potentials recorded intracellularly was 19.8 ± 0.6 msec ($n = 16$), more comparable with those evoked by spontaneous and synaptic inputs in anesthetized animals *in vivo* (see below; Chang, 1951a; Bishop and Clare, 1953; Purpura and Grundfest, 1956; Zhu and Sakmann, 1998). By depolarizing the membrane poten-

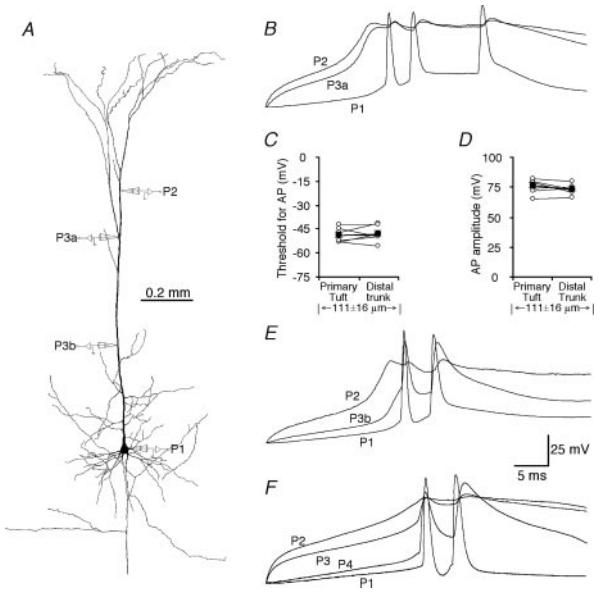

Figure 4. Propagation and spread of regenerative potentials along the apical dendrite. *A*, Schematic drawing of recording pipettes indicates the locations of the dendritic (809, 657, and 338 μm distal from the soma) and somatic recordings in two triple recordings from the same cell. The length of the apical dendrite was 1232 μm. *B*, Responses in the dendritic tufts (809 μm), distal dendritic trunk (657 μm), and soma to step-depolarizing current injections at the tufts of the same neuron. Note that the regenerative potential began first in the primary tufts, propagated to the distal dendritic trunk with little attenuation in amplitude, and was followed by the somatic action potentials. *C*, Threshold for dendritic regenerative potentials evoked by current injection in the primary tufts or distal trunks. *D*, Amplitude of dendritic regenerative potentials in the primary tufts and distal trunks in response to current injection in the primary tufts. *E*, Responses of the dendritic tufts (809 μm), proximal dendritic trunk (338 μm), and soma to step-depolarizing current injections at the tufts of the same neuron. Note that the regenerative potential started first in the primary tufts, propagated to the proximal dendritic trunk with intermediate attenuation in amplitude, and was followed by the somatic action potentials. The full-amplitude regenerative potentials in the proximal trunk were generated after the somatic action potentials. The resting membrane potential at the soma was −79 mV. The resting membrane potentials at the dendrite from distal to proximal were −68, −68, and −77 mV, respectively. *F*, Responses in a secondary dendritic tuft branch (*P2*; 869 μm), a primary dendritic tuft branch (*P3*; 706 μm), the proximal dendritic trunk (*P4*; 225 μm), and soma (*P1*) to step-depolarizing current injections at the distal tuft branch of another neuron. Note that the regenerative potential began first in the secondary tuft, propagated to the primary tuft with little attenuation in amplitude, and was followed by the full-amplitude regenerative action potentials first in the proximal dendrite and then in the soma. The resting membrane potential at the soma was −80 mV. The resting membrane potentials at the dendrite from distal to proximal were −68, −69, and −75 mV, respectively. The calibration applies to *B, E, F*.

tial in the dendrite, we found that the synaptic stimulation-evoked EPSP was followed by a slow inhibitory postsynaptic potential (Fig. 7*A,B*), which curtailed the duration of synaptically evoked dendritic potentials. The reversal potential of the slow potential, estimated by plotting its amplitude against the membrane potential, was −56.4 ± 2.9 mV ($n = 4$) (Fig. 7*B,C*), more depolarizing than the resting membrane potentials (cf. Zhu and Connors, 1999). These results suggest that the slow potential is generated by GABAergic inputs (Larkum et al., 1999a; Zhu and Connors, 1999; Porter et al., 2001), and it may contribute to the initial depolarization of the membrane potential and initiation of dendritic regenerative potentials. The peaks and dips of the dendritic regenerative potentials evoked by synaptic stimulation, representing back-propagating Na^+ action potentials initiated in the axon, were less evident. This is consistent with coactivation of disynaptic inhibitory potentials and a large increase in membrane conductance.

Initiation of dendritic regenerative potentials by synaptic stimulation of deep layers *in vitro*

Previous study has shown that back-propagating bursts of Na^+ action potentials induced by somatic current injections can evoke dendritic regenerative potentials (Larkum et al., 2001). We wished to know whether layer 4/5 synaptic inputs also could evoke bursts of somatic action potentials and, subsequently, regenerative potentials in the dendrite of layer 5 pyramidal neurons. Thus we made simultaneous recordings from layer 5 pyramidal neurons at the soma and tuft and examined their responses to the synaptic stimulation of layer 6. Unlike younger P14 neurons, which always responded to a suprathreshold somatic current injection with a single Na^+ action potential in the soma and a large back-propagating Na^+ action potential in the dendrite (Fig. 8*A*) (Stuart and Sakmann, 1994; Zhu, 2000), adult layer 5 pyramidal neurons responded to a suprathreshold somatic current injection with two different firing modes (Fig. 8*B,C*). Approximately one-half of them (22 of 43) responded with a single Na^+ action potential in the soma, which was followed by a small back-propagating Na^+ action potential in the dendrite, whereas the other one-half (21 of 43) responded with a burst of Na^+ action potentials at the soma, which was followed by a large Ca^{2+}-dependent regenerative potential in the dendrite. These results are consistent with the ideas that two populations [regular spiking (RS) and intrinsically bursting (IB) neurons (see Connors and Gutnick, 1990)] of large layer 5 pyramidal neurons exist in the adult neocortex and that they develop from a single population of young RS neurons (Franceschetti et al., 1998).

Although RS and IB cells fired action potentials in different modes, they had the same resting membrane potential (−77.4 ± 0.6 mV, $n = 17$ vs −77.2 ± 0.6 mV, $n = 18$; $p = 0.84$) and input resistance (19.3 ± 1.1 MΩ, $n = 17$ vs 20.6 ± 0.7 MΩ, $n = 18$; $p = 0.31$), consistent with a previous report (Chagnac-Amital et al., 1990). However, the morphology of these two populations of large layer 5 pyramidal neurons was different (Chagnac-Amital et al., 1990; Tseng and Prince, 1993). RS cells ($n = 18$) had a longer apical dendrite than IB cells ($n = 18$; 1256 ± 118 vs 1194 ± 71 μm; $p < 0.05$) but a slightly smaller soma (SA: 2613 ± 401 vs 2945 ± 616 μm^2; $p < 0.05$). The distance from the soma at which the apical dendrites form their main bifurcation was the same in RS cells and IB cells (0.58 ± 0.09, $n = 17$ vs 0.60 ± 0.09, $n = 18$; $p = 0.47$; the length of the apical dendrite was normalized as 1). The dendritic branch patterns of these cells and 16 P14 cells were quantified and compared by using the Sholl (1956) analysis (Fig. 8*D*). We found that RS cells had significantly fewer basal dendritic branches than IB cells ($p < 0.05$), whereas those of IB and P14 cells were the same ($p = 0.68$). RS and IB cells had the same number of apical dendritic branches ($p = 0.11$), which was significantly more than that of P14 cells ($p < 0.05$). These results indicate that the postnatal differentiation from a single population of large layer 5 pyramidal neurons into RS and IB cells is likely dependent on the maturation of both membrane and morphological properties.

We wanted to know whether intrinsic firing modes of layer 5 neurons affect the initiation of dendritic Ca^{2+}-dependent potentials. We first examined the initiation of dendritic Ca^{2+}-dependent

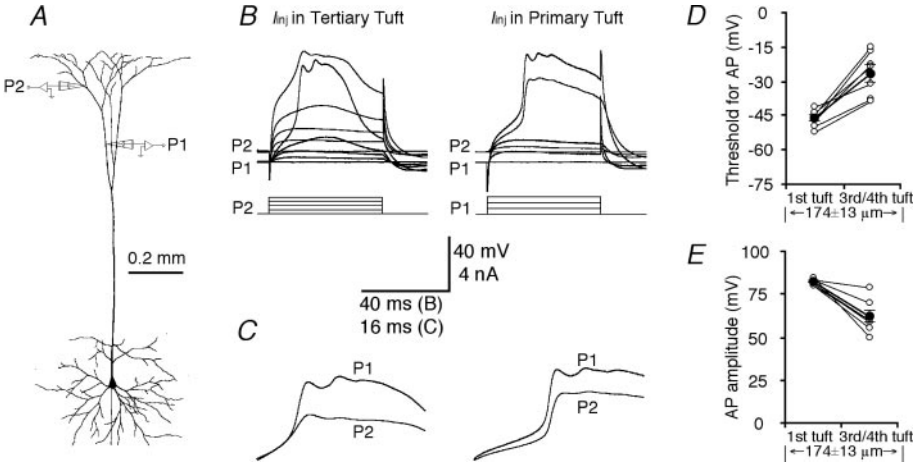

Figure 5. Initiation of the dendritic regenerative potentials in the apical dendritic tuft. *A*, The schematic drawing of recording pipettes indicates the locations of the dendritic recordings (867 and 1080 μm distal from the soma; primary and tertiary tufts, respectively). The length of the apical dendrite was 1210 μm. *B*, Responses to the step current injection in the primary or tertiary tufts. The suprathreshold recording traces are expanded and superimposed in *C* to show that the regenerative potentials always started earlier in the primary tufts. Note that the *top traces* show the responses in the tertiary tufts, whereas the bottom traces show the responses in the primary tufts. The resting membrane potentials at the primary and tertiary dendritic tufts were −68 and −62 mV, respectively. The calibration applies to both *B* and *C*. *D*, Threshold for dendritic regenerative potentials evoked by current injection in the primary and tertiary or quaternary tufts. *E*, Amplitude for dendritic regenerative potentials in the primary and tertiary or quaternary tufts in response to current injection in the primary tufts.

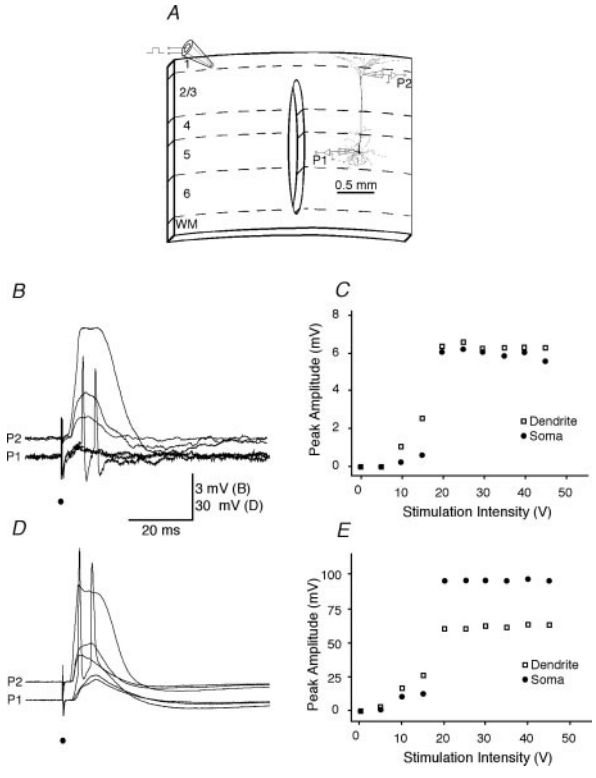

Figure 6. Layer 1 stimulation-evoked regenerative potentials in apical dendritic tuft. *A*, Schematic drawing of the preparation used to stimulate layer 1 input selectively (similarly in Fig. 7). The location of the dendritic recording was 1044 μm from the soma. The length of the apical dendrite was 1333 μm. *B*, Extracellular cell-attached recordings showed that synaptic stimulation-evoked regenerative potentials in the tufts started earlier than somatic action potentials. *C*, Average extracellular peak voltage responses (two trials) at the dendritic tufts and soma are plotted as a function of stimulation intensity. *D*, Intracellular recordings showed that regenerative potentials in the tufts started earlier than somatic action potentials. *E*, Average intracellular peak voltage responses (two trials) at the dendritic tufts and soma are plotted as a function of stimulation intensity. The calibration applies to *B* and *D*. The resting membrane potentials at the soma and dendrite were −80 and −74 mV, respectively.

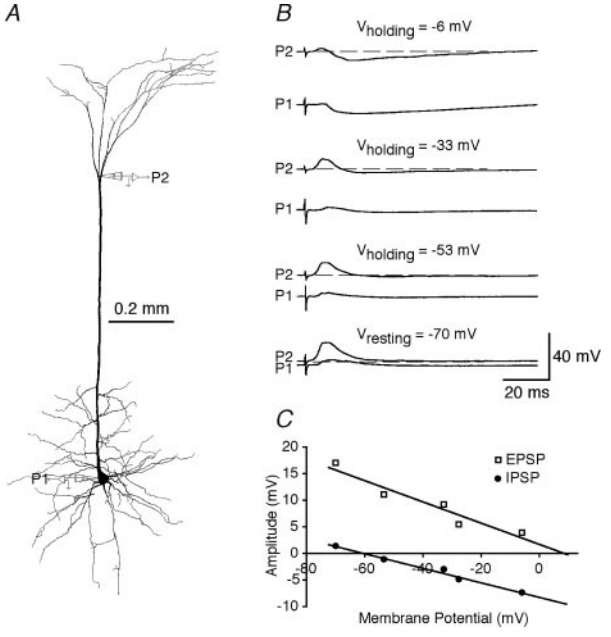

Figure 7. Layer 1 stimulation-evoked IPSP in apical dendritic tuft. *A*, The schematic drawing of recording pipettes indicates that the location of the dendritic recording was 914 μm from the soma. The length of the apical dendrite was 1300 μm. *B*, Intracellular recordings show the layer 1 stimulation-evoked EPSP and IPSP in the soma and tuft at different membrane potentials. The membrane potentials were altered by the injection of continuous depolarizing currents via the recording pipette in the tuft. *C*, Plot of amplitude of EPSP and IPSP against membrane potential in the tuft. The resting membrane potentials at the soma and dendrite were −74 and −70 mV, respectively.

potentials in RS and IB neurons by using long step current injections as stimuli (Fig. 8*E,F*). We found that a low-intensity current injection evoked tonic firing of Na^+ action potentials in the soma and a train of fast, small back-propagating action potentials in the dendrite of RS neurons. Increasing current intensity eventually could evoke a cluster or burst of two or more Na^+ action potentials at the onset of the response in the soma, followed by a large, slow Ca^{2+}-dependent potential in the dendrite of these neurons. In contrast, a low-intensity current injection evoked bursts of Na^+ action potentials in the soma and repetitive large, slow Ca^{2+}-dependent potentials in the dendrite of IB neurons. Increasing current injection intensity eventually could transform the later bursts into tonic firing of Na^+ action potentials in the soma, followed by a train of fast, small back-propagating action potentials in the dendrite of these neurons. We then examined the initiation of dendritic Ca^{2+}-dependent potentials in pyramidal neurons by

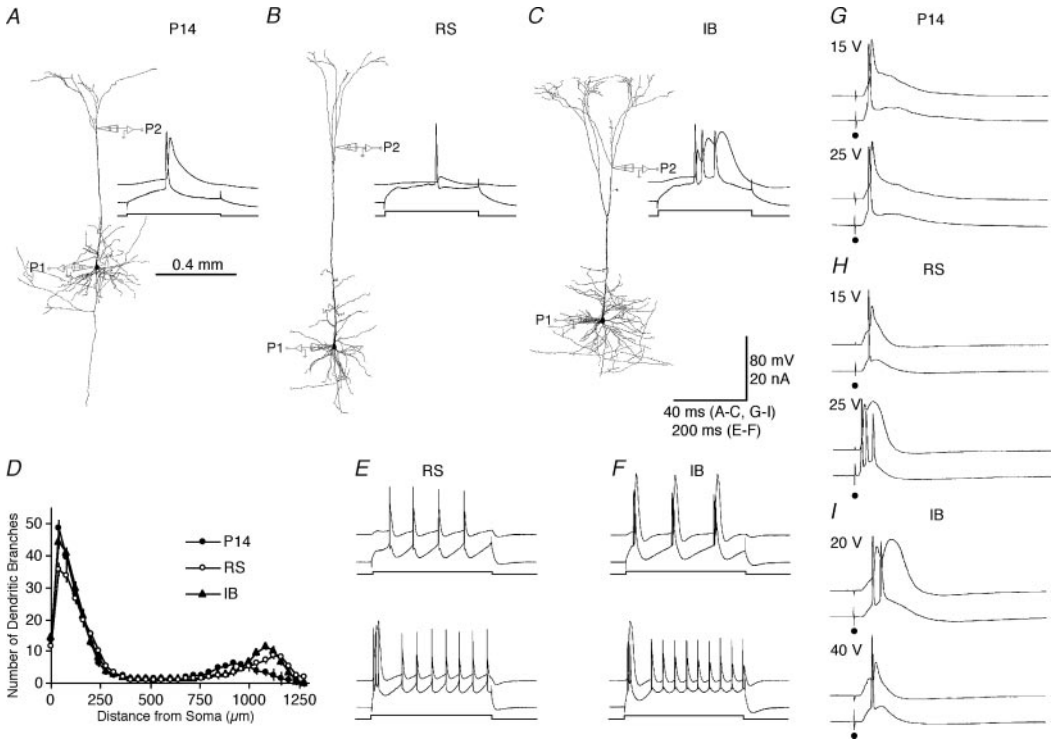

Figure 8. Synaptic stimulation-evoked regenerative potentials in apical dendritic tuft. *A*, Reconstruction of a biocytin-stained P14 pyramidal neuron. The schematic drawing of recording pipettes indicates the location of the dendritic (697 μm distal from the soma; secondary tufts) and somatic recordings. The length of the apical dendrite was 1002 μm. Threshold current injection into the soma induced a single action potential in the soma and a large, fast action potential in the tufts. The resting membrane potentials in the soma and dendrite were -66 and -68 mV, respectively. *B*, Reconstruction of a biocytin-stained RS pyramidal neuron. The schematic drawing of recording pipettes indicates the location of the dendritic (987 μm distal from the soma; secondary tufts) and somatic recordings. The length of the apical dendrite was 1469 μm. Threshold current injection into the soma induced a single action potential in the soma and a small, fast action potential in the tufts. The resting membrane potentials in the soma and dendrite were -69 and -76 mV, respectively. *C*, Reconstruction of a biocytin-stained IB pyramidal neuron. The schematic drawing of recording pipettes indicates the location of the dendritic (757 μm distal from the soma; secondary tufts) and somatic recordings. The length of the apical dendrite was 1222 μm. Threshold current injection into the soma induced a burst of action potentials in the soma and a large, slow action potential in the tufts. The resting membrane potentials in the soma and dendrite were -74 and -84 mV, respectively. *D*, Sholl analysis of dendritic branch patterns of P14 cells, RS cells, and IB neurons in layer 5. *E*, *Top traces*, A long current step injection induced repetitive action potentials in the soma and small, fast action potentials in the tufts in a RS neuron. Note that the amplitude of the fast action potentials in the tufts was reduced progressively. *Bottom traces*, Increasing the current intensity induced a burst of action potentials at the onset of in the response in the soma, which was followed by a large, slow calcium action potential in the tufts. The dendritic recording was 716 μm distal from the soma. The length of the apical dendrite was 1160 μm. The resting membrane potentials in the soma and dendrite were -60 and -81 mV, respectively. *F*, *Top traces*, A long current injection induced repetitive bursts in the soma and large, slow action potentials in the tufts in an IB neuron. *Bottom traces*, Increasing the current intensity transformed the later bursts into tonic-like firing, which was followed by small, fast action potentials in the tufts. Note that the amplitude of the fast action potentials in the tufts was reduced progressively. The dendritic recording was 870 μm distal from the soma. The length of the apical dendrite was 1231 μm. The resting membrane potentials in the soma and dendrite were -72 and -79 mV, respectively. *G*, Threshold and suprathreshold synaptic stimulation induced single action potentials in the soma and single large, fast action potentials in the tufts of a P14 cell. The dendritic recording was 590 μm distal from the soma. The length of the apical dendrite was 989 μm. The resting membrane potentials of the cell in the soma and dendrite were -72 and -75 mV, respectively. *H*, Threshold synaptic stimulation induced a single action potential in the soma and a small, fast action potential in the tufts of a RS cell. Suprathreshold synaptic stimulation induced a burst of action potentials in the soma and a large, slow action potential in the tufts of the RS cell. The dendritic recording was 907 μm distal from the soma. The length of the apical dendrite was 1420 μm. The resting membrane potentials of the cell in the soma and dendrite were -72 and -78 mV, respectively. *I*, Threshold synaptic stimulation induced a burst of action potentials in the soma and a large, slow action potential in the tufts of an IB cell. Suprathreshold synaptic stimulation induced a single action potential in the soma and a small, fast action potential in the tufts of the IB cell. The dendritic recording was 870 μm distal from the soma. The length of the apical dendrite was 1247 μm. The resting membrane potentials of the cell in the soma and dendrite were -71 and -77 mV, respectively.

using synaptic stimulations as stimuli (Fig. 8*G–I*). We found that, independent of synaptic stimulation intensity, synaptic stimulation of deep layers always evoked single Na^+ action potentials in the soma of P14 cells, followed by fast, large back-propagating action potentials in the tuft dendrite. RS cells fired a single action potential in the soma and a fast, small back-propagating action potential in the dendrite in response to a weak stimulus. Increasing stimulation intensity eventually could cause a burst of somatic action potentials in these cells and a large, slow Ca^{2+}-dependent potential in the dendrite. In contrast, IB cells fired a burst of action potentials in the soma and a large, slow Ca^{2+}-dependent potential in the dendrite in response in response to a weak stimulus. However, increasing stimulation intensity eventually could transfer the burst into a single action potential in the soma and a fast, small back-propagating action potential in the dendrite, attributable to the fact that IB cells receive more GABAergic inputs and that these inputs are activated only by strong stimuli (Chagnac-Amital et al., 1990; Tseng and Prince, 1993). These results indicate that back-propagating burst-evoked dendritic potentials signal somatic synaptic inputs differently in RS cells and IB cells.

In summary, we show here that layer 5 pyramidal neurons have a restricted action potential initiation zone in the apical dendrite,

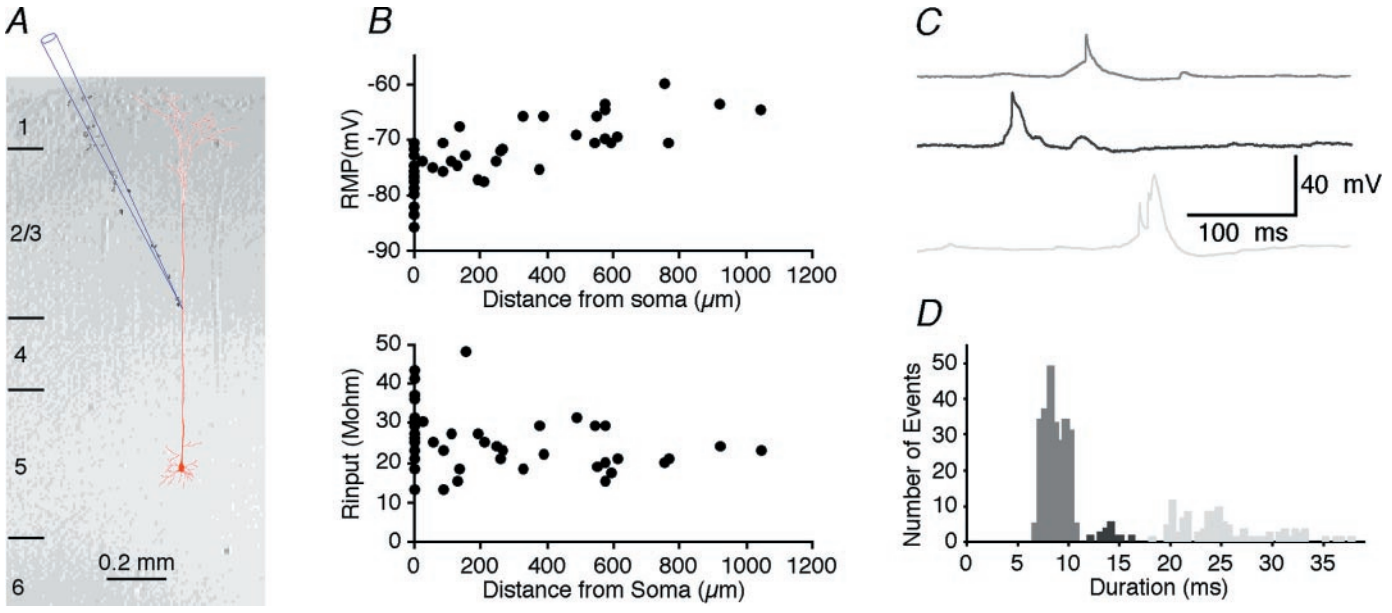

Figure 9. Spontaneous synaptic input-evoked dendritic regenerative potentials in the apical dendritic tuft. *A*, The schematic drawing of the recording pipette indicates the location of the dendritic recording (578 μm distal from the soma; dendritic trunk). Note the biocytin staining of cell debris (*black*) along the electrode penetration pathway (the same in the following figures). The length of the apical dendrite was 1370 μm. *B*, Plots of resting membrane potential and input resistance against distance from the soma of all layer 5 pyramidal neurons recorded *in vivo*. *C*, Spontaneous activity evoked three distinct forms of regenerative potentials in the layer 5 pyramidal neuron reconstructed in *A*. They were fast potential (*red*), slow potential (*blue*), and complex potential (*green*). *D*, Histogram of dendritic regenerative events with different duration. The resting membrane potential at the dendritic trunk was −64 mV.

which can be activated by layer 1 synaptic inputs to initiate a mainly Ca^{2+}-dependent action potential *in vitro*. These data combined with our previous reports complete the description of the apical dendrites in terms of the regenerative nature and location of the functionally different regions and their interaction with each other (Larkum et al., 1999a,b, 2001; Zhu, 2000). However, the question remains as to whether these forms of regenerative potentials recorded *in vitro* can be induced by synaptic or sensory inputs in the intact brain and whether their biophysical properties are altered, because certain physiological conditions in the intact brain can be quite different to *in vitro* ones. For example, a substantial proportion of the apical dendritic tree of layer 5 pyramidal neurons is trimmed in the thin brain slices, and it is likely that both excitatory and inhibitory circuits are impaired *in vitro*. In addition, spontaneous synaptic activity is prevalent in the intact brain (Zhu and Connors, 1999), and it is still poorly understood how this spontaneous activity affects the integration of distal synaptic inputs (Kamondi et al., 1998). Moreover, neuromodulators are being released continuously in the intact brain, and they are expected to modulate synaptic and dendritic properties to a great extent (Chen and Lambert, 1997; Wu and Saggau, 1997; Zhu and Heggelund, 2001). Therefore, we decided to make whole-cell recordings at the soma and different locations along the apical dendrite of layer 5 pyramidal neurons in the anesthetized rat to study the initiation and propagation of synaptic stimulation and whisker-evoked dendritic potentials.

Spontaneous activity-evoked dendritic regenerative potentials *in vivo*

Whole-cell recordings were made from the soma and apical dendrite of 53 layer 5 pyramidal neurons in anesthetized rats. The cell morphology of all 53 pyramidal neurons was recovered so that the exact recording sites from these neurons could be determined after the reconstruction of the electrode-advancing pathway (Fig. 9*A*). As with *in vitro* recordings (see above; Zhu, 2000; Berger et al., 2001), the resting membrane potential became progressively more depolarized when the recordings along the apical dendrite were made more and more distal from the soma, whereas the input resistance remained relatively constant along the apical dendrite (Fig. 9*B*).

Whole-cell *in vivo* recordings revealed numerous spontaneous synaptic inputs in the soma and apical dendrites of layer 5 pyramidal neurons (Fig. 9*C*). When the spontaneous EPSPs were large enough, they triggered regenerative potentials. In the apical dendrite three distinct forms of regenerative potentials were observed (Fig. 9*C*). The differences between these three potentials were seen best when the recordings were made from the corresponding dendritic action potential initiation zone determined *in vitro*. One form of regenerative potentials had a fast rising phase and a quick decaying phase (Fig. 9*C*, *top trace*), which we refer to as fast potentials. The second form rose quickly but decayed slowly (Fig. 9*C*, *middle trace*), and we refer to these as slow potentials. The third form of regenerative potentials appeared as a combination of a fast potential and a very slow potential with one to seven peaks and dips (Fig. 9*C*, *bottom trace*). We refer to these as complex potentials. These three regenerative potentials also could be separated according to their duration (Fig. 9*D*). Whereas fast potentials could last up to 10 msec, slow potentials ranged from 12 to 18 msec in the distal dendritic trunk and primary tuft branches. The duration of complex potentials varied significantly, ranging from 18 to 40 msec. This was attributable in part to the large variation in interval between the fast and slow component, ranging from 3.4 to 13.7 msec, and to the large difference in the number of peaks and dips they had. In four distal dendritic trunk or primary tuft recordings, over 300 spontaneous regenerative events were collected for each recording, and the relative occurrence of each form of regenerative poten-

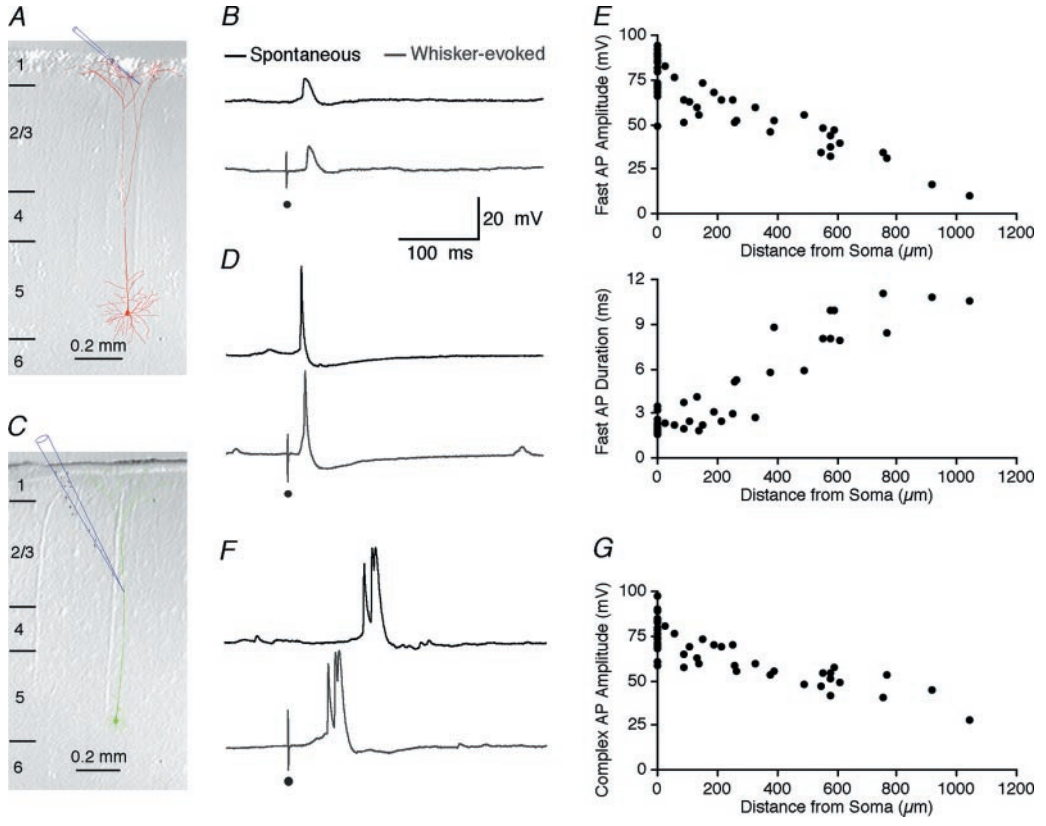

Figure 10. Spontaneous synaptic input and whisker-evoked fast and complex potentials in the apical dendritic tuft. *A*, The schematic drawing of the recording pipette indicates the location of the dendritic recording (1042 μm distal from the soma; tertiary tuft). The length of the apical dendrite was 1179 μm. *B*, Spontaneous input and whisker-evoked fast regenerative potentials in the layer 5 pyramidal neuron reconstructed in *A*. *C*, The schematic drawing of the recording pipette indicates the location of the dendritic recording (612 μm distal from the soma; dendritic trunk). The length of the apical dendrite was 1257 μm. *D*, Spontaneous input and whisker-evoked fast regenerative potentials in the layer 5 pyramidal neuron reconstructed in *C*. *E*, Plots of fast potential amplitude and duration against distance from the soma of all layer 5 pyramidal neurons recorded *in vivo*. *F*, Spontaneous input and whisker-evoked complex potentials in the layer 5 pyramidal neuron reconstructed in *C*. *G*, Plot of complex potential amplitude against distance from the soma of all layer 5 pyramidal neurons recorded *in vivo*. The resting membrane potentials at the tertiary tuft and dendritic trunk were −65 and −70 mV, respectively.

tials was quantified. Fast potentials were the most frequently observed regenerative events (69.4 ± 7.2%), followed by complex potentials (28.8 ± 7.5%). Slow potentials occurred at a very low incidence of 1.8 ± 0.7%.

Whisker-evoked fast and complex potentials *in vivo*

Depending on where the recordings were made, the amplitude and duration of fast potentials varied. They were smaller in amplitude and longer in duration when recorded from the tuft branches (Fig. 10*A,B*) but larger in amplitude and shorter in duration when recorded from the proximal dendritic trunk (Fig. 10*C,D*). There were linear correlations between the average amplitude ($r = 0.90$; $p < 0.0001$; $n = 53$; ANOVA) or average duration ($r = 0.91$; $p < 0.0001$; $n = 53$; ANOVA) of fast potentials and the distance from recording site to the soma (Fig. 10*E*). These results suggest that fast potentials originate from back-propagating Na^+ action potentials initiated in the axonal action potential initiation zone (Larkum et al., 2001). In addition to spontaneous inputs, a brief deflection of single whiskers frequently induced a fast potential (Fig. 10*B,D*). Because the ascending sensory inputs arrive primarily at layer 4 in anesthetized animals (Cauller and Kulics, 1988), such input would be expected to generated Na^+ potentials at the soma, which is consistent with the idea that fast potentials result from back-propagating Na^+ potentials. The small sample of distal dendritic recordings, however, does not allow us to validate whether the variability in amplitude of back-propagating potentials, reported by recent *in vitro* studies (Golding et al., 2001; Larkum et al., 2001), exists in the intact brain.

Sometimes a brief defection of whiskers induced a complex potential (Fig. 10*F*). This result, as well as the waveform of the potentials, suggests that complex potentials may result from bursts of back-propagating Na^+ action potentials and/or the interaction of single back-propagating Na^+ action potentials with synaptic inputs arriving at the dendritic action potential initiation zone (Fig. 8) (Larkum et al., 1999a,b). The maximum amplitude of the complex potentials decreased as a function of distance from the soma (Fig. 10*G*). At the distal dendritic trunk and low-order tuft branches their peak amplitude, dependent primarily on Ca^{2+} conductance (Larkum et al., 2001), remained relatively constant. This is consistent with our *in vitro* observation that a low-threshold zone with a high density of Ca^{2+} channels is present around the bifurcation region of the apical dendrite of layer 5 pyramidal neurons. The lone tertiary tuft recording gave a smaller complex potential, supporting our view that active conductances diminish in the terminal dendrite. The result is also consistent with the *in vivo* imaging result of reduced Ca^{2+} influx in the distal dendritic tips during the activation of dendritic regenerative potentials (Helmchen et al., 1999).

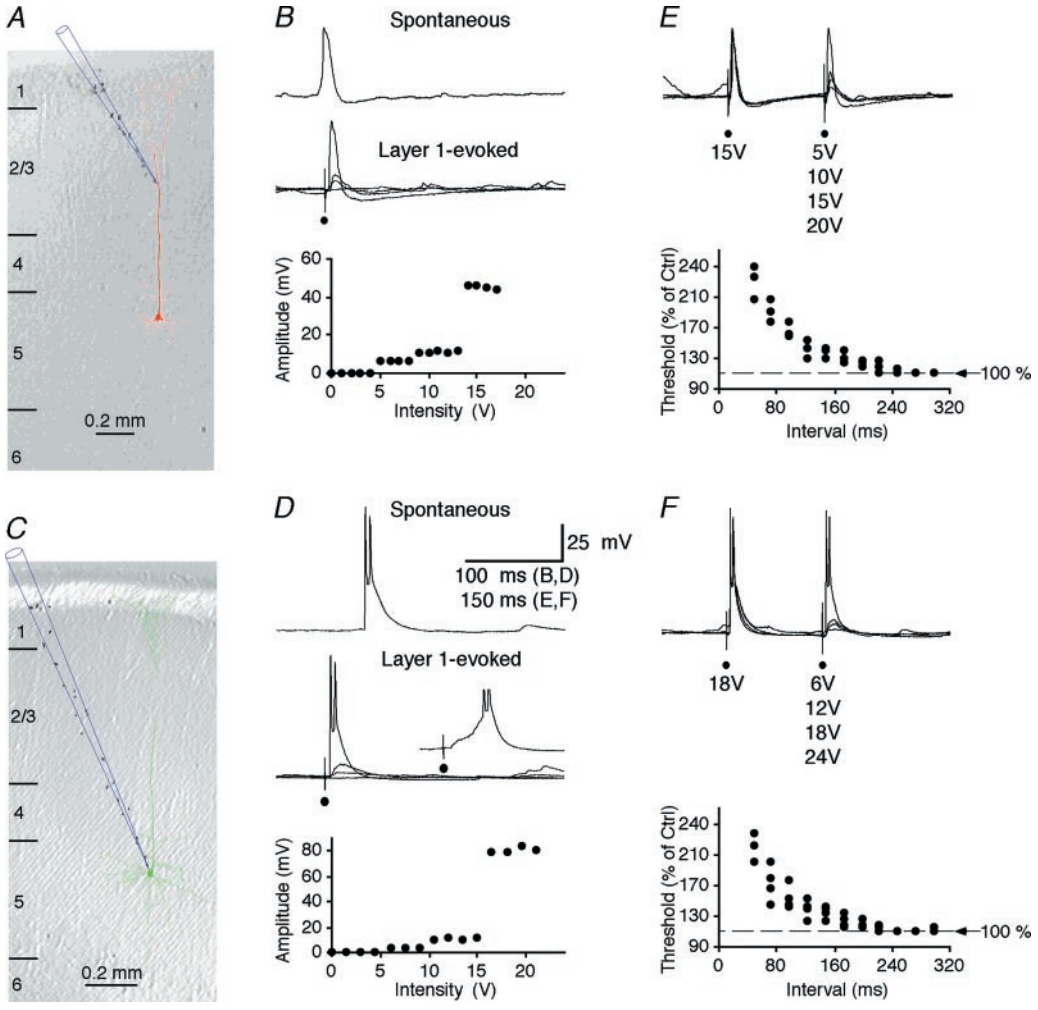

Figure 11. Spontaneous synaptic input and layer 1 stimulation-evoked slow potentials in the apical dendritic tuft. *A*, The schematic drawing of the recording pipette indicates the location of the dendritic recording (769 μm distal from the soma; primary tuft). The length of the apical dendrite was 1362 μm. *B*, Spontaneous input and layer 1 stimulation-evoked slow regenerative potentials in the layer 5 pyramidal neuron reconstructed in *A*. Shown is the plot of peak voltage response as a function of layer 1 stimulation intensity. *C*, The schematic drawing of the recording pipette indicates a somatic recording. The length of the apical dendrite was 1166 μm. *D*, Spontaneous input and layer 1 stimulation evoked a large, fast potential and burst of action potentials in the soma of the layer 5 pyramidal neuron reconstructed in *C*. The *inset* shows a whisker-evoked EPSP. Note the slow rise of the EPSP before it triggered a burst of sodium action potentials (sodium action potentials are truncated). Shown is the plot of peak voltage response as a function of layer 1 stimulation intensity. *E*, Paired layer 1 stimuli revealed the refractory period of the slow dendritic potential in the dendrite recorded from the layer 5 pyramidal neurons reconstructed in *A*. The *data points* in the plot were obtained from three different neurons. *F*, Paired layer 1 stimuli revealed the refractory period of the large fast potential recorded from the soma of the layer 5 pyramidal neurons reconstructed in *C*. The *data points* in the plot were obtained from four different neurons. The resting membrane potentials at the soma and dendrite were −71 and −65 mV, respectively.

Layer 1 stimulation-evoked slow potentials *in vivo*

Spontaneous slow potentials occurred rarely in anesthetized rats. Moreover, whisker deflections never induced any slow potential in our dendritic recordings. Because layer 1 inputs arrive at the distal tuft and they are suppressed in large part in anesthetized animals (Cauller and Kulics, 1988, 1991), we speculated that these inputs have a large influence on the initiation of slow potentials in the distal dendrite. We thus made recordings from the apical dendrite and stimulated the cortical surface directly to activate layer 1 fibers (Fig. 11*A*) (cf. Chang, 1951a). Cortical surface stimulation induced an EPSP, which could trigger a slow potential just like those spontaneously occurred ones (Fig. 11*B*). The evoked EPSP had a smooth, fast rising phase and exhibited little jittering in latency, suggesting a putative monosynaptic event. This result is consistent with the early suggestion that the response was attributable to the direct activation of the apical dendrite of layer 5 pyramidal neurons by layer 1 inputs (Chang, 1952). Interestingly, before reaching threshold, the EPSP showed a step-wise increase in amplitude in response to the increase of stimulating intensity, suggesting recruitment of presumably a small number of presynaptic fibers. On average, the activation of 4.7 ± 1.2 ($n = 3$) steps was required to trigger a slow potential in the dendrite of layer 5 pyramidal neurons in the intact brain.

To test how slow potentials affect the somatic firing, we used cortical surface stimulation while making recordings from the soma of layer 5 pyramidal neurons (Fig. 11*C*). Low-strength cortical surface stimulation induced an EPSP in the soma (Fig. 11*D*). When the stimulation reached the threshold, it triggered a large, fast rising potential and typically a burst of Na^+ action potentials. The average number of Na^+ action potentials in the bursts was 1.8 ± 0.2 ($n = 12$). Occasionally, similar large and fast potentials occurred as spontaneous events (Fig. 11*D*). The quick

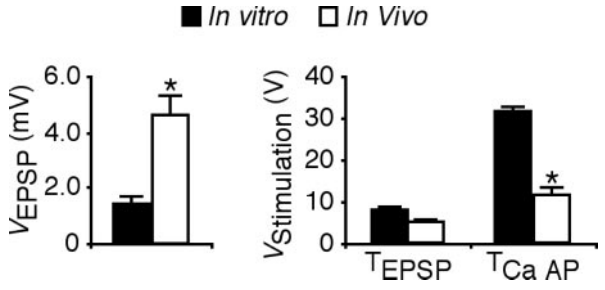

Figure 12. Threshold and amplitude of synaptic responses in the apical dendrite *in vitro* and *in vivo*. *Left*, Amplitude of minimal evoked EPSP recorded in the apical dendrite *in vitro* and *in vivo*. *Right*, Threshold for evoked dendritic EPSPs and Ca^{2+}-dependent regenerative potentials *in vitro* and *in vivo*. $^*p < 0.05$ (Student's *t* test).

rising phase of these potentials distinguished them from those spontaneous or whisker-evoked bursts that ride on a slow EPSP (Fig. 11*D*, *inset*). Like slow potentials recorded in the dendrite, cortical surface stimulation also induced a step-wise increase in amplitude of the response, with 4.3 ± 0.7 ($n = 7$) activation steps required to trigger a large, fast depolarization and burst firing. This threshold is the same as the one for inducing slow potentials in the dendrite ($p > 0.5$), indicating that slow dendritic potentials originate from the activation of layer 1 fibers in the cortex and that they evoke a large depolarization and a burst of Na^+ action potentials at the soma of layer 5 pyramidal neurons. These results also predict that slow dendritic potentials and large, fast rising somatic depolarization are more frequent events in awake animals, because layer 1 inputs are enhanced dramatically in that behavioral state (Cauller and Kulics, 1988, 1991). Although the regenerative potentials initiated in the distal dendrite always actively propagate in the distal trunk *in vitro*, recordings also show that they can either propagate actively or spread passively to the soma along the proximal dendrite (Figs. 3*B*, 4) (see also Larkum et al., 2001). However, the fast rising phase of large somatic potentials recorded *in vivo* suggests that slow potentials propagate actively all the way along the apical dendrite to the soma in the intact brain.

The refractory period of cortical surface stimulation-evoked potentials was examined by using paired stimuli (Fig. 11*E,F*). Paired stimuli with varying intervals showed that the second stimulus often failed to evoke a regenerative potential if the interval was too short. Varying the interval of two stimuli and stimulation intensity of the second stimulus revealed a relative refractory period of ~250 msec for the slow potentials in the dendrite ($n = 3$) and large, fast potentials in the soma ($n = 4$). This refractory period is the same as that of the regenerative potentials initiated in the distal dendrite *in vitro* (Fig. 2*F*). The results supports the view that the slow potentials in the dendrite and large, fast potentials in the soma are attributable to the activation of layer 1 inputs and distal dendritic action potential initiation zone.

There was a notable difference between synaptically evoked responses in the dendrite *in vivo* and *in vitro* (Fig. 12). Although the threshold for inducing synaptic responses was the same *in vivo* and *in vitro* (5.3 ± 0.3 V, $n = 6$ vs 7.8 ± 0.9 V, $n = 16$; $p = 0.10$), the minimal EPSP evoked by the threshold stimulus was significantly larger *in vivo* than *in vitro* (4.56 ± 0.76 mV, $n = 6$ vs 1.43 ± 0.26 mV, $n = 16$; $p < 0.0005$), with the amplitude ranging from 2.11 to 7.17 mV *in vivo* and from 0.56 to 4.31 mV *in vitro*. Because single presynaptic axons can make multiple synapses on the different dendritic branches of single postsynaptic pyramidal neurons (Lisman and Harris, 1993), one possible explanation for the result is that some of the synapses made by single layer 1 fibers on the tuft branches of layer 5 pyramidal neurons are removed when the apical dendrite tree is trimmed during slicing. Consistent with the idea, we found that the threshold for activation of dendritic regenerative potentials was significantly lower *in vivo* than *in vitro* (11.5 ± 1.8 V, $n = 6$ vs 31.3 ± 1.5 V, $n = 16$; $p < 0.0005$). Further study is required to confirm this idea and/or to determine other mechanisms that may be responsible for the difference.

DISCUSSION

Our *in vitro* experiments demonstrate that the apical dendrite of adult (> P42) thick-tufted pyramidal neurons in cortical layer 5 has a low-threshold region for the initiation of mostly Ca^{2+}-dependent regenerative potentials. This zone is situated in the apical dendrite ~550–900 μm from the soma, including typically the distal dendritic trunk and the primary and secondary tufts. In *in vitro* conditions, dendritic regenerative potentials can be restricted locally to the distal dendritic arbor without inducing somatic firing, but more frequently they propagate actively for some distance, then either continuously travel actively or spread passively along the proximal dendrite toward the soma, where they induce a burst of two to four action potentials. Our *in vivo* experiments confirm that layer 1 inputs can activate the dendritic action potential initiation zone and evoke regenerative potentials propagating actively toward the soma, where they induce one to three Na^+ action potentials. In addition, back-propagating Na^+ action potentials by themselves or by interacting with the dendritic action potential initiation zone evoke fast and complex potentials in dendrite *in vivo*. Sensory inputs from whiskers trigger either a fast potential or a complex potential when they reach threshold.

Multiple forms of dendritic potentials

Previous studies have shown that active conductances, such as Na^+ and Ca^{2+} conductances, are present in the apical dendrite of pyramidal neurons (Huguenard et al., 1989; Stuart and Sakmann, 1994; Yuste et al., 1994; Magee and Johnston, 1995b; Markram et al., 1995; Kavalali et al., 1997). The initial phase of dendritic potentials is predominantly Na^+-dependent because it is blocked by TTX (Larkum et al., 2001). The slower phase of regenerative potentials is mediated primarily by Ca^{2+} conductances (Zhu, 2000; Larkum et al., 2001). As with younger neurons (Wei et al., 2001), the distribution of high-density active conductances extends to the primary and secondary tuft branches, because regenerative potentials can be induced in these branches with low threshold. Interestingly, the density of active conductances in the very distal dendrites (i.e., the tertiary and quaternary tufts) appears reduced when compared with the bifurcation region, suggesting a more passive membrane for the dendritic terminals. This result explains the reduced Ca^{2+} influx observed in the distal dendritic tips during the activation of dendritic regenerative potentials *in vivo* (Helmchen et al., 1999).

Although dendritically initiated regenerative potentials often forward-propagate and depolarize the axonal action potential initiation zone reliably to give rise to a burst of action potentials *in vitro*, there are conditions under which they can be restricted locally without inducing somatic firing (Larkum et al., 2001).

However, in the intact brain, slow dendritic potentials propagate reliably to the soma because suprathreshold layer 1 inputs evoke all-or-none potentials in both distal dendrite and soma with the same threshold. More interestingly, judged by the fast rising phase of the layer 1 input-evoked large depolarization in the soma, slow dendritic potentials appear to propagate actively all the way to the soma *in vivo*, whereas only approximately one-half of neurons do so *in vitro* (Larkum et al., 2001). This result suggests that the *in vivo* condition is more favorable for active propagation of dendritic potentials (cf. Rhodes and Llinas, 2001). This may be attributable to the intact circuit *in vivo*, which generates stronger, more synchronized spontaneous and evoked excitatory and inhibitory inputs in postsynaptic neurons than *in vitro*. Although these synaptic inputs would be expected to decrease the amplitude of regenerative potentials by increasing membrane conductance, they also would be expected to facilitate the activation of regenerative currents by shortening the membrane time constant. In addition, a higher temperature (37°C *in vivo* vs 35°C *in vitro*) also may contribute somewhat to the reliable propagation, because calcium channel kinetics are highly sensitive to the temperature ($Q_{10} \cong 3$; Coulter et al., 1989; McAllister-Williams and Kelly, 1995). Indeed, changing the temperature in the recording chamber from 35 to 30°C is enough to result in a large increase in membrane input resistance and a transformation of forward-propagating dendritic potentials into locally restricted ones without inducing somatic firing *in vitro* [our unpublished data; see also Wei et al. (2001) for locally restricted potentials recorded at room temperature], consistent with these ideas. It is worthwhile noting that dendritic regenerative potentials recorded in the immature tuft dendrites *in vitro* often are restricted locally and tend not to induce somatic firing (Schiller et al., 1997; Zhu, 2000), attributable in part to fewer active channels available in the initiation zone at this developmental stage (Zhu, 2000). However, it remains to be determined whether the regenerative potentials initiated in young tufts can cause a depolarization large enough to induce somatic Na^+ action potentials in the intact brain.

Besides locally initiated slow potentials, active conductances in the distal dendrite support single back-propagating fast potentials, which may be mediated primarily by Na^+ channels (Stuart and Sakmann, 1994; Larkum et al., 2001). The complex potentials recorded in this study are likely to be dependent on the activation of both Na^+ and Ca^{2+} channels (Larkum et al., 1999a,b, 2001). Because a large amount of Ca^{2+} influx is detected around the bifurcation range of the apical dendrite when burst firing is induced at the soma of layer 5 pyramidal neurons by depolarizing current injection or spontaneous activity (Helmchen et al., 1999), some of the complex potentials probably result from back-propagating bursts of Na^+ action potentials (Fig. 8) (Larkum et al., 1999b). However, back-propagating bursts are unlikely to be responsible for all complex potentials because some complex potentials recorded *in vivo* can have an interval between the fast and slow component >13 msec, and it is possible for the back-propagating bursts of Na^+ of action potentials to initiate complex potentials only when their intraburst frequency surpasses a critical frequency (i.e., >80 Hz; Larkum et al., 1999b). Thus some of the complex potentials are more likely to have been produced by the interaction of single back-propagating Na^+ of action potentials and distal subthreshold synaptic inputs (Larkum et al., 1999a). Clearly, more *in vivo* experiments are needed to determine the origin of complex potentials.

Functional significance

The properties of dendritically initiated regenerative potentials are very different from axonal ones. Therefore, the two initiation sites of pyramidal cells most likely have different functions in neuronal signaling. Dendritic regenerative potentials have a 10- to 20-fold longer duration than Na^+-dependent axonal action potentials and much longer (~20-fold) absolute and relative refractory periods. This long refractory period would allow suprathreshold repetitive excitatory signals arriving in the tuft dendrites to be "transmitted" to the soma only at a relatively low frequency.

Alternatively, the apical dendrites may function as a "mode switch" for different output action potential patterns. The main inputs to dendritic tufts are from the higher-order cortical areas (Zeki and Shipp, 1988; Felleman and Van Essen, 1991; Johnson and Burkhalter, 1997; Cauller et al., 1998), cholinergic and monoaminergic nuclei (De Lima and Singer, 1986; Lysakowski et al., 1986), and secondary ascending sensory system (Herkenham, 1979; Casagrande, 1994; Jones, 1998). These inputs can generate a prolonged depolarization in their target neurons (Benardo, 1993; Shao and Burkhalter, 1996). The long-lasting depolarizations (Fig. 1*B*) (Zhu, 2000), together with the intrinsic (Silva et al., 1991; Amitai, 1994) and synaptic (Reyes and Sakmann, 1999) properties of adult layer 5 pyramidal neurons, may promote bursts at alpha rhythm for a short period. Because the alpha rhythm may be related to mechanisms of attention (Ray and Cole, 1985; Vanni et al., 1997), one speculation is that distal synaptic inputs are used to form an "attentional/select" window (Squire and Zola-Morgan, 1991; Olshausen et al., 1993). Namely, when layer 1 attentional signals "switch" a group of layer 5 pyramidal neurons into the burst firing mode, they secure that salient and/or ambiguous sensory information from layer 4 input is amplified in these cells and relayed to their target cells (Lisman, 1997; Williams and Stuart, 1999; Zhu, 2000). This notion is supported by the finding that layer 1 activity is suppressed in sleeping animals but dramatically enhanced in alert animals (Cauller and Kulics, 1988). Thus the dendritic regenerative potential initiation zone may play a key role in attention-related information processing.

Back-propagating action potential-evoked fast and complex potentials may be important for transferring somatic information back to the distal dendrite. In the young animals single Na^+ action potentials back-propagate to the distal dendrite without much reduction in their amplitude (Stuart and Sakmann, 1994). These large back-propagating signals appear to be critical for the induction of synaptic plasticity, such as the long-term potentiation between layer 5 pyramidal neurons (Markram et al., 1997). However, single back-propagating Na^+ action potentials can produce only a very small depolarization (Fig. 10) and cause little Ca^{2+} influx in the adult tuft dendrites (Helmchen et al., 1999), and they appear not to be effective in inducing long-term potentiation in adult pyramidal neurons (Thomas et al., 1998; Pike et al., 1999). Thus the maturation of the dendritic action potential initiation zone (Zhu, 2000) and back-propagating burst-evoked complex potentials may be crucial for the efficient induction of long-term synaptic plasticity in the adult distal dendrite of layer 5 pyramidal neurons by back-propagating signals.

REFERENCES

Amitai Y (1994) Membrane potential oscillations underlying firing patterns in neocortical neurons. Neuroscience 63:151–161.

Amitai Y, Friedman A, Connors BW, Gutnick MJ (1993) Regenerative activity in apical dendrites of pyramidal cells in neocortex. Cereb Cortex 3:26–38.

Benardo LS (1993) Characterization of cholinergic and noradrenergic

slow excitatory postsynaptic potentials from rat cerebral cortical neurons. Neuroscience 53:11–22.
Benardo LS, Masukawa LM, Prince DA (1982) Electrophysiology of isolated hippocampal pyramidal dendrites. J Neurosci 2:1614–1622.
Berger T, Larkum ME, Lüscher H-R (2001) High I_h channel density in the distal apical dendrite of layer 5 pyramidal cells increases bidirectional attenuation of EPSPs. J Neurophysiol 85:855–868.
Bishop GH, Clare MH (1953) Responses of cortex to direct stimuli applied at different depths. J Neurophysiol 16:1–19.
Casagrande VA (1994) A third parallel visual pathway to primary area V1. Trends Neurosci 17:305–310.
Cauller LJ, Connors BW (1994) Synaptic physiology of horizontal afferents to layer I in slices of rat SI neocortex. J Neurosci 14:751–762.
Cauller LJ, Kulics AT (1988) A comparison of awake and sleeping cortical states by analysis of the somatosensory-evoked response of postcentral area 1 in rhesus monkey. Exp Brain Res 72:584–592.
Cauller LJ, Kulics AT (1991) The neural basis of the behaviorally relevant N1 component of the somatosensory-evoked potential in SI cortex of awake monkeys: evidence that backward cortical projections signal conscious touch sensation. Exp Brain Res 84:607–619.
Cauller LJ, Clancy B, Connors BW (1998) Backward cortical projections to primary somatosensory cortex in rats extend long horizontal axons in layer I. J Comp Neurol 390:297–310.
Chagnac-Amital Y, Luhmann HJ, Prince DA (1990) Burst-generating and regular-spiking layer 5 pyramidal neurons of rat neocortex have different morphological features. J Comp Neurol 296:598–613.
Chang H-T (1951a) Dendritic potential of cortical neurons as produced by direct electrical stimulation of the cerebral cortex. J Neurophysiol 14:1–21.
Chang H-T (1951b) Changes in excitability of cerebral cortex following single electric shock applied to cortical surface. J Neurophysiol 14:95–111.
Chang H-T (1952) Cortical and spinal neurons: cortical neurons with particular reference to the apical dendrites. Cold Spring Harbor Symp Quant Biol 17:189–202.
Chapin JK, Lin CS (1984) Mapping the body representation in the SI cortex of anesthetized and awake rats. J Comp Neurol 229:199–213.
Chen H, Lambert NA (1997) Inhibition of dendritic calcium influx by activation of G-protein-coupled receptors in the hippocampus. J Neurophysiol 78:3484–3488.
Chen WR, Midtgaard J, Shepherd GM (1997) Forward and backward propagation of dendritic impulses and their synaptic control in mitral cells. Science 278:463–467.
Connors BW, Gutnick MJ (1990) Intrinsic firing patterns of diverse neocortical neurons. Trends Neurosci 13:99–104.
Coulter DA, Huguenard JR, Prince DA (1989) Calcium currents in rat thalamocortical relay neurones: kinetic properties of the transient, low-threshold current. J Physiol (Lond) 414:587–604.
De Lima AD, Singer W (1986) Cholinergic innervation of the cat striate cortex: a choline acetyltransferase immunocytochemical analysis. J Comp Neurol 250:324–338.
Dykes RW, Dudar JD, Tanji DG, Publicover NG (1977) Somatotopic projections of mystacial vibrissae on cerebral cortex of cats. J Neurophysiol 40:997–1014.
Felleman DJ, Van Essen DC (1991) Distributed hierarchical processing in the primate cerebral cortex. Cereb Cortex 1:1–47.
Franceschetti S, Sancini G, Panzica F, Radici C, Avanzini G (1998) Postnatal differentiation of firing properties and morphological characteristics in layer 5 pyramidal neurons of the sensorimotor cortex. Neuroscience 83:1013–1024.
Golding NL, Spruston N (1998) Dendritic sodium spikes are variable triggers of axonal action potentials in hippocampal CA1 pyramidal neurons. Neuron 21:1189–1200.
Golding NL, Jung HY, Mickus T, Spruston N (1999) Dendritic calcium spike initiation and repolarization are controlled by distinct potassium channel subtypes in CA1 pyramidal neurons. J Neurosci 19:8789–8798.
Golding NL, Kath WL, Spruston N (2001) Dichotomy of action-potential backpropagation in CA1 pyramidal neuron dendrites. J Neurophysiol 86:2998–3010.
Hausser M, Spruston N, Stuart GJ (2000) Diversity and dynamics of dendritic signaling. Science 290:739–744.
Helmchen F, Svoboda K, Denk W, Tank DW (1999) *In vivo* dendritic calcium dynamics in deep-layer cortical pyramidal neurons. Nat Neurosci 2:989–996.
Herkenham M (1979) The afferent and efferent connections of the ventromedial thalamic nucleus in the rat. J Comp Neurol 183:487–517.
Huguenard JR, Hamill OP, Prince DA (1989) Sodium channels in dendrites of rat cortical pyramidal neurons. Proc Natl Acad Sci USA 86:2473–2477.
Johnson RR, Burkhalter A (1997) A polysynaptic feedback circuit in rat visual cortex. J Neurosci 17:7129–7140.
Jones EG (1998) Viewpoint—the core and matrix of thalamic organization. Neuroscience 85:331–345.
Kamondi A, Acsady L, Buzsaki G (1998) Dendritic spikes are enhanced by cooperative network activity in the intact hippocampus. J Neurosci 18:3919–3928.
Kavalali ET, Zhuo M, Bito H, Tsien RW (1997) Dendritic Ca^{2+} channels characterized by recordings from isolated hippocampal dendritic segments. Neuron 18:651–663.
Kim HG, Connors BW (1993) Apical dendrites of the neocortex: correlation between sodium- and calcium-dependent spiking and pyramidal cell morphology. J Neurosci 13:5301–5311.
Larkum ME, Zhu JJ, Sakmann B (1999a) A new cellular mechanism for coupling inputs arriving at different cortical layers. Nature 398:338–341.
Larkum ME, Kaiser KMM, Sakmann B (1999b) Calcium electrogenesis in distal apical dendrites of layer 5 pyramidal cells at a critical frequency of back-propagating action potentials. Proc Natl Acad Sci USA 96:14600–14604.
Larkum ME, Zhu JJ, Sakmann B (2001) Dendritic mechanisms underlying the coupling of the dendritic with the axonal AP initiation zone of adult layer 5 pyramidal neurons. J Physiol (Lond) 533:447–466.
Lisman JE (1997) Burst as a unit of neural information: making unreliable synapses reliable. Trends Neurosci 20:38–43.
Lisman JE, Harris KM (1993) Quantal analysis and synaptic anatomy—integrating two views of hippocampal plasticity. Trends Neurosci 16:141–147.
Lysakowski A, Wainer BH, Rye DB, Bruce G, Hersh LB (1986) Cholinergic innervation displays strikingly different laminar preferences in several cortical areas. Neurosci Lett 64:102–108.
Magee JC (2000) Dendritic integration of excitatory synaptic input. Nat Rev Neurosci 1:181–190.
Magee JC, Johnston D (1995a) Synaptic activation of voltage-gated channels in the dendrites of hippocampal pyramidal neurons. Science 268:301–304.
Magee JC, Johnston D (1995b) Characterization of single voltage-gated Na^+ and Ca^{2+} channels in apical dendrites of rat CA1 pyramidal neurons. J Physiol (Lond) 487:67–90.
Markram H, Helm PJ, Sakmann B (1995) Dendritic calcium transients evoked by single back-propagating action potentials in rat neocortical pyramidal neurons. J Physiol (Lond) 485:1–20.
Markram H, Lübke J, Frotscher M, Sakmann B (1997) Regulation of synaptic efficacy by coincidence of postsynaptic APs and EPSPs. Science 275:213–221.
McAllister-Williams RH, Kelly JS (1995) The temperature dependence of high-threshold calcium channel currents recorded from adult rat dorsal raphe neurones. Neuropharmacology 34:1479–1490.
Oakley JC, Schwindt PC, Crill WE (2001) Initiation and propagation of regenerative Ca^{2+}-dependent potentials in dendrites of layer 5 pyramidal neurons. J Neurophysiol 86:503–513.
Olshausen BO, Anderson CH, Van Essen DC (1993) A neurobiological model of visual attention and invariant pattern recognition based on dynamic routing of information. J Neurosci 13:4700–4719.
Pike FG, Meredith RM, Olding AW, Paulsen O (1999) Postsynaptic bursting is essential for "Hebbian" induction of associative long-term potentiation at excitatory synapses in rat hippocampus. J Physiol (Lond) 518:571–576.
Porter JT, Johnson CK, Agmon A (2001) Diverse types of interneurons generate thalamus-evoked feedforward inhibition in the mouse barrel cortex. J Neurosci 21:2699–2710.
Purpura PD, Grundfest H (1956) Nature of dendritic potentials and synaptic mechanisms in cerebral cortex of cat. J Neurophysiol 19:573–595.
Ray WJ, Cole HW (1985) EEG alpha activity reflects attentional demands, and β-activity reflects emotional and cognitive processes. Science 228:750–752.
Regehr W, Kohoe J, Ascher P, Armstrong C (1993) Synoptically triggered action potentials in dendrites. Neuron 11:145–151.
Reyes A (2001) Influence of dendritic conductances on the input–output properties of neurons. Annu Rev Neurosci 24:653–675.
Reyes A, Sakmann B (1999) Developmental switch in the short-term modification of unitary EPSPs evoked in layer 2/3 and layer 5 pyramidal neurons of rat neocortex. J Neurosci 19:3827–3835.
Rhodes PA, Llinas RR (2001) Apical tuft input efficacy in layer 5 pyramidal cells from rat visual cortex. J Physiol (Lond) 536:167–187.
Schiller J, Schiller Y, Stuart G, Sakmann B (1997) Calcium action potentials restricted to the distal apical dendrites of rat neocortical pyramidal neurons. J Physiol (Lond) 505:605–616.
Schwindt PC, Crill WE (1995) Amplification of synaptic current by persistent sodium conductance in apical dendrite of neocortical neurons. J Neurophysiol 74:2220–2224.
Schwindt PC, Crill WE (1998) Synaptic evoked dendritic action potentials in rat neocortical pyramidal neurons. J Neurophysiol 79:2432–2446.
Shao Z, Burkhalter A (1996) Different balance of excitation and inhibition in forward and feedback circuits of rat visual cortex. J Neurosci 16:7353–7365.
Sholl DA (1956) The organization of the cerebral cortex. London: Methuen.
Silva LR, Amitai Y, Connors BW (1991) Intrinsic oscillations of neocortex generated by layer 5 pyramidal neurons. Science 251:432–435.

Simons DJ (1983) Multi-whisker stimulation and its effects on vibrissa units in rat SmI barrel cortex. Brain Res 276:178–182.
Spencer WA, Kandel ER (1961) Electrophysiology of hippocampal neurons. IV. Fast potentials. J Neurophysiol 26:272–285.
Squire LR, Zola-Morgan S (1991) The medial temporal lobe memory system. Science 253:1380–1386.
Stuart G, Sakmann B (1994) Active propagation of somatic action potentials into neocortical pyramidal cell dendrites. Nature 367:69–72.
Stuart G, Schiller J, Sakmann B (1997) Action potential initiation and propagation in rat neocortical pyramidal neurons. J Physiol (Lond) 505:617–632.
Thomas MJ, Watabe AM, Moody TD, Makhinson M, O'Dell TJ (1998) Postsynaptic complex spike bursting enables the induction of LTP by theta frequency synaptic stimulation. J Neurosci 18:7118–7126.
Tseng GF, Prince DA (1993) Heterogeneity of rat corticospinal neurons. J Comp Neurol 335:92–108.
Turner RW, Meyers DER, Richardson TL, Barker JL (1991) The sites for initiation of action potential discharge over the somatodendritic axis of rat hippocampal neurons. J Neurosci 11:2270–2280.
Vanni S, Revonsuo A, Hari R (1997) Modulation of the parieto-occipital alpha rhythm during object detection. J Neurosci 17:7141–7147.
Wei D-S, Mei Y-A, Bagal A, Kao JPY, Thompson SM, Tang C-M (2001) Compartmentalized and binary behavior of terminal dendrites in hippocampal pyramidal neurons. Science 293:2272–2275.
Williams SR, Stuart GJ (1999) Mechanisms and consequences of action potential burst firing in rat neocortical pyramidal neurons. J Physiol (Lond) 521:467–482.
Wong RK, Stewart M (1992) Different firing patterns generated in dendrites and somata of CA1 pyramidal neurones in guinea-pig hippocampus. J Physiol (Lond) 457:675–687.
Wong RK, Prince DA, Basbaum AI (1979) Intradendritic recordings from hippocampal neurons. Proc Natl Acad Sci USA 76:986–990.
Wu LG, Saggau P (1997) Presynaptic inhibition of elicited neurotransmitter release. Trends Neurosci 20:204–212.
Yuste R, Gutnick MJ, Saar D, Delaney KR, Tank DW (1994) Ca^{2+} accumulations in dendrites of neocortical pyramidal neurons: an apical band and evidence for two functional compartments. Neuron 13:23–43.
Zeki S, Shipp S (1988) The functional logic of cortical connections. Nature 335:311–317.
Zhu JJ (2000) Maturation of layer 5 neocortical pyramidal neurons: amplifying salient layer 1 and layer 4 inputs by Ca^{2+} action potentials in adult rat tuft dendrites. J Physiol (Lond) 526:571–587.
Zhu JJ, Connors BW (1999) Intrinsic firing patterns and whisker-evoked synaptic responses of neurons in the rat barrel cortex. J Neurophysiol 81:1171–1183.
Zhu JJ, Heggelund P (2001) Muscarinic regulation of axonal and dendritic outputs of rat thalamic interneurons: a new cellular mechanism for uncoupling distal dendrites. J Neurosci 21:1148–1159.
Zhu JJ, Sakmann B (1998) Whisker-evoked slow oscillation (7–12 Hz) in single neurons of the rat barrel cortex. Soc Neurosci Abstr 24:1512.